

# RESEARCH MEMORANDUM

INVESTIGATION OF DOWNWASH AND WAKE CHARACTERISTICS

AT A MACH NUMBER OF 1.53. I - RECTANGULAR WING

By Edward W. Perkins and Thomas N. Canning

Ames Aeronautical Laboratory  
Moffett Field, Calif.

CLASSIFICATION CANCELLED

Authority NACA R7 2411 Date 8/18/54

By MDA 8/31/54 See \_\_\_\_\_

CLASSIFIED DOCUMENT

This document contains classified information affecting the National Defense of the United States within the meaning of the Espionage Act, USC 50:31 and 32. Its transmission or the revelation of its contents in any manner to an unauthorized person is prohibited by law. Information so classified may be imparted only to persons in the military and naval services of the United States, appropriate civilian officers and employees of the Federal Government who have a legitimate interest therein, and to United States citizens of known loyalty and discretion who of necessity must be informed thereof.

## NATIONAL ADVISORY COMMITTEE FOR AERONAUTICS

WASHINGTON  
March 1, 1949

UNCLASSIFIED



NACA LIBRARY

AMES AERONAUTICAL LABORATORY



UNCLASSIFIED

## NATIONAL ADVISORY COMMITTEE FOR AERONAUTICS

RESEARCH MEMORANDUM

## INVESTIGATION OF DOWNWASH AND WAKE CHARACTERISTICS AT A

MACH NUMBER OF 1.53. I - RECTANGULAR WING

By Edward W. Perkins and Thomas N. Canning


## SUMMARY

The results of an experimental investigation of the downwash and wake characteristics behind a rectangular plan-form wing in a supersonic stream are presented. The aspect ratio of the wing was 3.5, and the airfoil section was a 5-percent-thick, symmetrical, double wedge with maximum thickness at 50-percent chord. The tests were made at a Mach number of 1.53 and a Reynolds number, based on the wing chord length, of approximately 1.25 million.

A comparison has been made between the downwash angles predicted by the linear theory and the measured downwash angles. The experimental trends of the variation of downwash angle with angle of attack at zero lift in the spanwise, streamwise, and vertical directions were similar to those predicted by the linear theory, but in most instances the experimental values were slightly greater than those given by theory. The comparison also showed that the displacement of the vortex sheet and the resulting influence on the downwash distribution must be considered in calculating downwash angles at finite angles of attack.

For the low-aspect-ratio wing used in this investigation, the distortion of the vortex sheet behind the wing-tip region had a considerable influence on the position of the wake and on the downwash distribution within a large portion of the induced flow field. In the region outboard of approximately the 30-percent semispan station, the distortion of the vortex sheet decreased the displacement of the sheet considerably from the value calculated by the linear theory.

The general characteristics of the friction wake were similar to those observed in subsonic flow. With increasing distance behind the wing, the wake expanded slowly, decreased in intensity, and, with



UNCLASSIFIED

the wing at positive angles of attack, moved downward relative to the free-stream direction.

## INTRODUCTION

A rational approach to the longitudinal-stability problem of supersonic aircraft requires knowledge of the downwash field behind a lifting surface. Theoretical methods for treatment of this problem have been developed and applied to a limited number of cases. (See references 1 and 2.) In accordance with the usual assumptions of the linearized theory, valid applications of these solutions are limited to thin wings at vanishingly small angles of attack. In addition, since the theory assumes that the fluid is inviscid, the effects of the wake are neglected.

At subsonic speeds, theoretical downwash calculated by means of a simplified lifting-line theory has yielded satisfactory agreement with experiment only when modified to account for both the displacement of the shed vortex sheet and the effects of the wake. The necessary empirical modifications to the basic theory were determined as the result of a number of experimental investigations. (See reference 3.) Similarly, in supersonic flow, experiment must be depended upon to determine the limits of applicability of the linearized inviscid theory. At present, there are only two published reports, which are readily available, dealing with experimental investigations of the induced flow field behind lifting surfaces in supersonic flow (references 4 and 5); in neither instance has a comparison been made with the theory now available.

In order to provide a comparison with the predictions of the linear theory, a general investigation of the downwash and wake behind several wing plan forms has been undertaken at the Ames Aeronautical Laboratory. The present report presents the results for a rectangular wing.

## SYMBOLS

c	wing chord, inches
s	wing semispan, inches
$\alpha$	wing angle of attack, degrees
H	free-stream total pressure, pounds per square inch absolute

- $\Delta H^*$  difference between the pitot pressure at a point in the wake and the pitot pressure in the free stream, pounds per square inch absolute (The pitot pressure is the pressure measured by a pitot tube in either subsonic flow, where this pressure is equal to the local total pressure, or in supersonic flow, where this pressure is equal to the local total pressure of the flow behind a normal shock wave.)
- $e$  downwash angle measured from the free-stream direction, degrees
- $e'$  downwash angle referred to the flow angle at  $\alpha=0$ , degrees
- $x, y, z$  longitudinal, lateral, and normal coordinates with the origin at the leading edge of the root section and the  $x$  axis corresponding to the free-stream direction.

## APPARATUS AND TESTS

### Wind Tunnel

The experimental investigation was performed in the Ames 1- by 3-foot supersonic wind tunnel No. 1, which is a closed-return, variable-pressure tunnel. A more complete description of the wind tunnel and associated equipment is contained in reference 6. The Mach number within the test section of the fixed nozzle was approximately 1.53.

### Model and Support

The model used for the tests was a semispan model of a rectangular wing of aspect ratio 3.5 with a 5-percent-thick, symmetrical, double-wedge section with maximum thickness at 50-percent chord. The dimensions of the wing and its orientation on the support plate are shown in figure 1. The wing surfaces were ground smooth but were not polished. The leading and trailing edges were finished to 0.001-inch radius and the wing tip was cut off parallel to the free-stream direction with no wing-tip fairing. Thus the 5-percent-thick double-wedge section was continuous over the entire span.

The model was mounted on a thin circular plate, termed the boundary-layer plate, positioned in the stream so as to by-pass the tunnel-wall boundary layer between the plate and the tunnel sidewall. (See fig. 1.) With this method of mounting, the area of the wing

which was influenced by the boundary-layer flow along the plate was considerably less than if the wing had been mounted on the tunnel wall, for only the relatively thin boundary layer which started at the upstream edge of the plate influenced the flow over the model. This plate was tapered in the streamwise direction so that the boundary-layer by-pass channel expanded in the downstream direction; as a result, supersonic flow was maintained in the channel.

Since the determination of the induced flow field behind a lifting wing requires accurate measurement of small flow deflections and, consequently, a stream which is free of disturbances other than those due to the lifting surface itself, the following precautions were taken to minimize possible interference due to the model-support system:

1. The test-section side of the boundary-layer plate was ground flat to a tolerance of  $\pm 0.002$  inch.
2. The entire circumference of the plate was beveled on the by-pass-channel side to a sharp knife-edge as indicated in figure 1.
3. The plate was alined as closely as possible with the free-stream direction in order to reduce the intensity of the pressure disturbance from the supersonic portion of the leading edge.

However, from the results of static-pressure surveys made parallel to the free-stream direction in a horizontal plane which included the tunnel axis, a small disturbance which passed across the outer portion of the wing was known to exist. The results of these pressure surveys and the location and magnitude of the pressure disturbance are described in more detail in reference 7.

#### Instrumentation

Measurements of the change in the local downwash angles with angle of attack of the airfoil were made with two different devices: a  $30^\circ$  cone with two pressure orifices symmetrically disposed, one on top and one on the bottom, and a  $10^\circ$  wedge with five sets of symmetrically disposed orifices. (See fig. 2.)

In order to make simple, direct comparisons between the experimental and theoretical values of  $dc/d\alpha$ , the measurement of the downwash angles should be point measurements. However, any set of orifices on the wedge indicates a stream angle which is dependent on the stream-angle variation over that part of the leading edge of the wedge included within the Mach forecones from the orifices. Thus, in

a region where the stream-angle gradient along the wedge was changing, only an average value of the stream angle was obtained from each set of orifices. For the wedge, the length of leading edge included within the Mach forecones from a set of orifices is approximately 18 percent of the wing semispan. In order to reduce this source of inaccuracy and to approach more closely a point measurement of the stream angle, a cone was substituted for the wedge. For the cone, the effective length included within the Mach forecones of the orifices is less than 2 percent of the wing semispan. Comparison of stream-angle measurements made with the cone and wedge showed that either instrument was suitable for measuring stream angles.

Actually two cones were mounted on a horizontal traverse bar as shown in figure 2(a), thus enabling the determination of the spanwise distribution of downwash angle in two planes above the extended chord plane of the wing during each test. The sets of orifices on the wedge were located at 10, 30, 50, 70, and 90 percent of the wing semispan. The wedge and lower cone were mounted 0.35 wing chord length above the extended chord plane of the wing; whereas the upper cone was mounted 0.70 chord length above the extended chord plane.

At each angle of attack of the airfoil the instruments were pitched so as to obtain zero pressure difference between the symmetrically disposed orifices. Thus, the change in the angle of null pressure difference and the corresponding change in wing angle of attack are  $\Delta\epsilon$  and  $\Delta\alpha$ , respectively.

The viscous wake of the wing was surveyed with a rake of pitot tubes. (See fig. 2(b).) The rake consisted of 39 pitot tubes with 0.05-inch vertical spacing mounted on a vertical support blade. The tubes were placed alternately on each side of the blade so that a spacing of 0.10 inch was maintained between tubes. This was believed adequate to avoid possible interference between adjacent tubes, since it is estimated that the minimum Mach number in the wake at the survey stations was sufficiently supersonic to preclude any mutual interference effects which might have influenced the pressures at adjacent tubes. The support blade was mounted on a traverse bar similar to that used for the cones, thus permitting a complete spanwise survey at each of the two wake-survey stations. Each of the tubes in the rake was connected to a tube in a multiple-tube manometer filled with tetrabromoethane, and the pitot-pressure profiles were recorded by photographing the manometer board.

### Test Methods

In these tests, the model was considered to be the wing in a conventional configuration of wing-tail combination with the stream-angle measuring device substituted for the usual tail surface at various positions above the extended chord plane and downstream of the trailing edge. The positions of the four downwash survey stations and two wake survey stations are shown in figure 1. These stations were placed, in a manner, compatible with the support system, so as to provide a measure of the downwash field in the vicinity of the most probable tail location.

With the wing installed and a stream-angle measuring device mounted as shown in figure 3, the angle of attack of the wing was varied between the limits of  $\pm 10^\circ$ , and the resulting changes in downwash angle at the survey points determined. The pitot-pressure profiles were obtained at each of the two wake survey stations (stations 5 and 6) for angles of attack of the wing of  $0^\circ$ ,  $3^\circ$ ,  $6^\circ$ , and  $9^\circ$ .

All tests were made at a tunnel total pressure of 18 pounds per square inch absolute which gives a test Reynolds number of approximately 1.25 million based on the wing chord. The specific humidity of the air was maintained below 0.0003 pound of water per pound of dry air, a value at which condensation effects are negligible.

### REDUCTION OF THE DATA

#### Downwash

Since the angle of attack of the model was changed by rotating the entire support system, it was necessary to apply corrections to the data obtained with the wing in place to account for both the flow deflections induced by rotation of the support system and the nonuniformity of the free stream. At each survey point, the changes in local stream angle accompanying changes in angle of attack of the model support system with no model in place were measured for an angle-of-attack range of  $\pm 10^\circ$ . The results of these stream calibrations, which were used in reduction of the data as point-by-point corrections, showed:

1. At station 1 ( $x=2c$ ,  $z=0.35c$ ) stream-angle changes were negligible throughout the angle-of-attack range.
2. At station 2 ( $x=3c$ ,  $z=0.35c$ ) a maximum stream angle of  $0.3^\circ$

was measured near the support plate. This deflection decreased with increasing distance from the support plate to less than  $0.1^\circ$  at the 90-percent-semispan point.

3. An incomplete calibration, not suitable for use in making corrections, was obtained at station 3 ( $x=3c$ ,  $z=0.70c$ ).

4. At station 4 ( $x=4.43c$ ,  $z=0.35c$ ) near the support plate, a deflection of  $1.4^\circ$  at  $-10^\circ$  angle of attack was measured. This deflection decreased almost linearly to  $0^\circ$  at  $\alpha=0^\circ$ . In the positive angle range the deflection increased linearly to  $0.2^\circ$  at  $\alpha=7^\circ$ . Deflections in both ranges decreased with increasing distance from the support plate.

It can be seen from these results that the principal interference from the support system was confined within the Mach cones from the subsonic portion of the leading edge of the boundary-layer plate (fig. 3) and that the interference was smallest near the Mach cone surface and increased as the Mach cone axis was approached. These stream calibrations were used to correct the data at all the survey stations except station 3. In view of the relative positions of stations 2 and 3, it is believed that at station 3 the interference from the support system would be only slightly greater than at station 2. Since the corrections at station 2 are small and have little effect on the final results, it is concluded that the uncorrected results presented for station 3 are qualitatively useful.

The evaluation of  $de/d\alpha$  does not require a measurement of the downwash angle referred to the free-stream direction, but only an evaluation of the change in downwash angle with change in angle of attack. Therefore, the values of the stream angle presented are based on the assumption of zero downwash at zero angle of attack and thus have been indicated as  $\epsilon'$ .

#### Wake

The wake was located by determining its position relative to the survey rake from photographs of the manometer board and computing the position of the rake relative to the wing from the known geometry of the system. The limit of the wake was arbitrarily defined as the point at which  $\Delta H'/H$  is equal to  $-0.005$ . The quantity  $\Delta H'$  is the difference between the pitot pressure at a point in the wake and the pitot pressure in the free stream and  $H$  is the free-stream total pressure. Since no instrument was available to measure the static-pressure variation in the wake, it was impossible to determine



the Mach number or velocity profiles through the wake.

#### PRECISION

The following consideration of the possible sources of inaccuracy in the determination of the downwash angle indicates an estimated possible error of  $\pm 0.10^\circ$  in any one downwash angle. These sources of error are:

1. Stream-angle variation in the undisturbed stream at the position of the wing
2. Sensitivity of the stream-angle instruments
3. Measurement of the stream angle both for stream calibration and for tests with the wing in place
4. Measurement of the angle of attack of the wing

The effect of the stream-angle variation in the undisturbed stream at the position of the wing as well as possible errors arising from the sensitivity of the stream-angle instruments are considered negligible throughout the angle-of-attack range. Measurement of all angles, that is, stream angle with the wing out or in place and the wing angle of attack, were made with a vernier protractor with a least count of  $0.1^\circ$ . If a possible error of one-half of the least count is assumed for each of these angles and the square root of the sum of the squares of these assumed errors is taken in accordance with the method of reference 8, the total possible error in  $\epsilon'$  is slightly less than  $\pm 0.10^\circ$ . On this basis, the possible error in determining  $(d\epsilon/d\alpha)_{\alpha=0}$  is slightly less than  $\pm 0.04$ .

In determining the profiles of pitot-pressure loss in the wake, the principal sources of error are:

1. Inexact pressure measurements due to unavoidable differences in the shape of tube openings (No attempt has been made to evaluate this error, but it is believed to be small.)
2. The observed bending of individual total-head tubes, which introduces an estimated error of  $\pm 0.025$  inch in the location of any particular plotted point in the profile
3. The 0.05-inch vertical spacing of the tubes, which gives an estimated possible error in location of the wake limits

with respect to the rake of  $\pm 0.025$  inch

4. The possible inaccuracy in measuring the position of the rake relative to the wing, which is estimated as  $\pm 0.05$  inch

The sum of errors 1 and 2 is sufficiently large to justify fairing the curves without passing through each point. The square root of the sum of the squares of errors 2, 3, and 4 yields a total estimated possible error in location of the wake of  $\pm 0.061$  inch or  $\pm 0.021$  chord length.

### THEORY

In the application of linearized theory to the problem of determining the characteristics of the induced flow field behind a lifting surface, the surface is considered to be at infinitesimally small angles of attack so that it is contained completely in the  $xy$  plane with the  $x$  axis corresponding to the free-stream direction. The trailing vortex sheet is assumed to lie in the plane of the wing and to extend unchanged to infinity. However, under lifting conditions this simplified picture must be altered to account for the self-induced movement of the vortex system. In subsonic flow (reference 3), it has been found that the shed vortex sheet is rapidly displaced downward and deformed so that it curves into a channel of constantly increasing depth and distends rapidly as it proceeds to roll up like a volute about the tip vortex cores. It has been shown that for purposes of predicting the average downwash over a tail surface for conventional wing-tail combinations in subsonic flow, the rolling up of the trailing vortex sheet may be neglected. Satisfactory agreement between experiment and theory may be obtained if the trailing vortex sheet is considered to be displaced vertically by an amount equal to the displacement of the center line of the actual distorted vortex sheet. This displacement is readily calculated since the vortex sheet passes through the trailing edge of the airfoil and its inclination is everywhere equal to the downwash angle at that point. Thus, at a point  $p$

$$(\Delta z)_p = -\tan \alpha \int_c^{x_p} \left( \frac{d\epsilon}{d\alpha} \right)_{\substack{z=0 \\ y=\text{const.}}} dx - c \tan \alpha$$

For the particular arrangement employed in these tests, wherein the points at which the downwash angles were to be determined were always above the extended chord plane, the change in displacement of

the vortex sheet accompanying changes in the angle of attack was such that the distance between the survey point and the point of maximum downwash at the vortex sheet (wake center line) decreased with increasing angle of attack. Thus, since the linear theory shows that  $d\epsilon/d\alpha$  increases as the vortex sheet is approached, it follows that the slope of the theoretical curves of the variation of  $\epsilon$  with  $\alpha$  would increase as  $\alpha$  is increased. If the movement of the vortex sheet is assumed to be that predicted by theory, an approximation to the nonlinear increase in downwash may be calculated by means of the theory in a manner similar to that employed in reference 3. The calculation of  $\epsilon$  at angle of attack  $\alpha$  for each survey point is accomplished by evaluating the theoretical displacement of the vortex sheet at the xy coordinates of the survey point. From this value of the displacement, the distance between the survey point and the displaced vortex sheet can be determined. With a knowledge of this distance and the theoretical variation of  $d\epsilon/d\alpha$  with distance from the vortex sheet (reference 1), a value of  $d\epsilon/d\alpha$ , and hence  $\epsilon$ , can be calculated.

Calculations of this nature have been performed for each of the survey points and the results have been plotted in figure 4. The approach used to obtain these curves was different from the method used for subsonic flow in reference 3 in that the displacement of the vortex sheet at each of the spanwise survey points was evaluated and used to calculate the resulting change in  $d\epsilon/d\alpha$  at that point rather than basing the change in  $d\epsilon/d\alpha$  on the displacement of the vortex sheet at the plane of symmetry.

## DISCUSSION

### Downwash

The results of the measurement of the downwash angles for various spanwise positions at four survey stations, which were above the extended chord plane and downstream from the trailing edge of the wing, are plotted in figure 4. The curves showing the theoretical variation of  $\epsilon$  with  $\alpha$ , computed in the manner previously described, are shown for comparison. There is no appreciable difference between the slopes of these theoretical curves at  $\alpha=0$  and the values of  $(d\epsilon/d\alpha)_{\alpha=0}$  computed by the methods presented in reference 1, which do not account for the movement of the vortex sheet. Therefore, these curves may be used for a comparison of the experimental results and the theoretical predictions of reference 1.

The experimental results show that at any semispan position  $(d\epsilon/d\alpha)_{\alpha=0}$  increases with increasing distance downstream from the trailing edge and decreases with increasing distance above the extended chord plane as the theory predicts. At station 1 the agreement between the theory and the experimental results is very good over the entire angle-of-attack range tested except at the 10-percent-semispan position. At survey stations 2, 3, and 4, relatively good agreement is obtained at the 10- and 30-percent-semispan positions. However, at the 50- and 70-percent-semispan positions the experimental results differ considerably from the theoretical values, particularly at positive angles of attack. Both the linear theory and the experimental results show that the value of  $d\epsilon/d\alpha$  at the survey points increases as the angle of attack is increased. However, the increase in  $d\epsilon/d\alpha$  between  $-10^\circ$  and the maximum positive angle of attack, shown by the experimental results, is greater than predicted by the linear theory. In each instance,  $d\epsilon/d\alpha$  increases more rapidly in the positive angle-of-attack range and decreases more rapidly with increasing negative angle of attack than the linear theory predicts. This phenomenon is consistent with the results which will be shown later, wherein the vortex sheet behind the wing-tip region generally moves downward less rapidly with increasing positive angle of attack than the theory predicts. Thus, as the angle of attack is increased in the positive angle-of-attack range, the vortex sheet is closer to the survey points than the theory predicts. Consequently, the downwash at each of these points is greater than the theoretical. Conversely, in the negative angle-of-attack range, the vortex sheet is farther from the survey point than the theory predicts and the downwash is less than the theoretical.

At the 90-percent-semispan positions, even though the displacement of the vortex sheet is different from that predicted by theory, little effect on the downwash is felt over a large angle-of-attack range, because both the experimental results and the theory indicate that  $d\epsilon/d\alpha$  is equal to zero for a considerable distance above and below the survey points. Therefore, changes in distance between the survey points and the wake center line will have little effect on the downwash predicted and measured at this spanwise position for a considerable angle-of-attack range. At stations 1, 2, and 3, the experimental results show practically zero downwash at negative angles of attack. At station 2, there is a sharp break in the experimental data between  $\alpha=2-1/2^\circ$  and  $\alpha=5^\circ$  followed by a portion of the curve that indicates decreasing downwash. This break is probably associated with the position of the wing-tip vortex relative to the survey instrument; however, sufficient data are not

available to analyze the flow conditions.

Two additional factors which would tend to cause the downwash to depart from that predicted by linear theory for finite angles of attack may be suggested as follows:

1. Interaction between shock wave and boundary layer at trailing edge.— Ferri (reference 9) has shown that shock-wave boundary-layer interaction can cause separation of the boundary layer ahead of the trailing edge on the low-pressure surface of a lifting wing. This flow separation is accompanied by a loss in lifting pressure between the separation point and trailing edge, and, in addition, by a movement of the origin of the trailing vortex sheet. The calculations of the downwash angles at finite angles of attack are based on the assumption that the trailing edge is the origin of the vortex sheet. However, the flow separation on the low-pressure side of the airfoil would cause the origin of the vortex sheet to be displaced from the trailing edge to the low-pressure side of the airfoil and would thus change the effective vertical location of any point in the flow field from that assumed in the theoretical analysis.

2. Detachment of the leading-edge shock wave.— It can be seen from the experimental results that at large negative angles of attack there was a large decrease in  $d\epsilon/d\alpha$  at most of the survey points. This decrease may be the result of the distortion of the vortex sheet previously considered. However, an additional factor which may contribute to the observed decrease is the detachment of the leading-edge shock wave. For the 5-percent-thick, double-wedge airfoil section used for this wing, the leading-edge shock wave detaches at an angle of attack of approximately  $9.5^\circ$  at a free-stream Mach number of 1.53. This shock-wave detachment may result in a redistribution of the downwash within the induced flow field which may in turn result in a decrease in the downwash at the survey point. However, it should be pointed out that no net decrease in downwash over the entire induced flow field would be anticipated since experimental results for a similar rectangular wing (reference 10) have shown that, not only does the lift continue to increase at angles of attack greater than that for which the shock wave detaches, but also the lift-curve slope continues to increase.

#### Wake

The pitot pressure-loss profiles presented in figure 5 indicate the location, thickness, and intensity of the wake for several

semispan positions at survey stations 5 and 6 which were 3.3 and 5.0 chord lengths aft of the leading edge, respectively. The horizontal reference line used in this figure is a line drawn in the free-stream direction through the leading edge of the airfoil. As can be seen from this plot, the general characteristics of the wake are similar to those observed in subsonic flow. With the wing at a positive angle of attack, the wake expands slowly, decreases in intensity, and moves downward relative to the free-stream reference line with increasing distance behind the wing. In the spanwise direction the intensity of the wake was greatest at the 10-percent-semispan station and least at the 90-percent station; whereas, at the three intermediate stations, the wake was of approximately equal intensity. In general, the spanwise variation of the wake thickness was similar.

A spanwise plot of the upper limit of the wake (fig. 6) reflects both the wake-thickness distribution and the integrated effects of the downwash on the wake position. Although the wake appears to be higher at station 5 than at station 6 at  $\alpha=0^\circ$ , this difference in height is within the experimental accuracy of the measurements. Since the wake expands slowly between the two stations, the upper surface of the wake is probably slightly higher at station 6. The greater thickness of the wake behind the wing root causes the upper limit of the wake to be somewhat higher at the root than at the tip. In addition, since the vertical location of the wake at any spanwise position is determined by the variation in the stream direction from the wing leading edge to the survey position of the downwash at the vortex sheet, the wake will be higher behind the root than behind the tip at survey stations 5 and 6 because of the difference in the streamwise variation of downwash angle. A considerable region of zero downwash exists at the vortex sheet behind the trailing edge of the root section, since, in accordance with the theoretical considerations of reference 1, the downwash is zero at all points which are behind the plane wave from the trailing edge and outside the Mach cone from the leading-edge tip. No comparable region of zero downwash is found behind the tip. Therefore, since the wake follows the downwash, it is apparent that for small distances behind the airfoil the displacement of the wake will be greatest behind the tip and least behind the root. It should be noted that in figure 6 the position of the wake is referred to the extended chord plane of the wing rather than a plane parallel to the free stream and passing through the leading edge of the wing to which the displacement is normally referred.

The position of the wake center line, which is assumed to be coincident with the shed vortex sheet, has been determined experimentally at various angles of attack at survey stations 5 and 6.

The results are plotted in figure 7 for comparison with the positions calculated by means of the linear theory. The accuracy of the experimental determination of the position of the wake center line is relatively poor, being only about  $\pm 2$  percent of the wing chord. The agreement obtained between experiment and theory in the vertical plane of symmetry indicates that the linear theory may be used to determine the wake location in the plane of symmetry at these distances behind the wing. However, outboard of approximately the 30-percent-semispan position, the agreement is poor. In this region, the experimental results show that the vortex sheet was displaced from the free-stream direction by an amount which was less than that predicted by the theory. Since the wake must follow the downwash, it is apparent that in this region the downwash at the vortex sheet is less than that predicted by theory. However, no actual measurements were made in the wake to support this contention. The shape of the curve defining the position of the wake center line in the region behind the wing tip suggests that the rolling-up process is beginning to take place.

#### CONCLUDING REMARKS

The results obtained in this investigation indicate that the methods presented in reference 1 are sufficient for determining  $dc/d\alpha$  at  $\alpha=0$ . However, the displacement of the vortex sheet and the resulting effects on the downwash distribution must be considered in calculating downwash angles at finite angles of attack. In addition, it appears that the displacement and distortion of the vortex sheet in the region behind the wing tip has considerable influence on the downwash distribution within a large portion of the induced flow field.

The results also indicate that the linear theory can be used to calculate the displacement of the wake, or shed vortex sheet, at the vertical plane of symmetry at distances behind the wing comparable to the test range. In the region outboard of approximately 30 percent of the wing semispan, the distortion of the vortex system decreases the displacement of the sheet considerably from the values calculated by the linear theory.

Ames Aeronautical Laboratory,  
National Advisory Committee for Aeronautics,  
Moffett Field, Calif.

## REFERENCES

1. Lagerstrom, P. A., and Graham, Martha E.: Downwash and Sidewash Induced by Three-Dimensional Lifting Wings in Supersonic Flow. Douglas Aircraft Co., Inc., Rep. No. SM-13007, Apr. 1947.
2. Heaslet, Max. A., and Lomax, Harvard: The Calculation of Downwash Behind Supersonic Wings With an Application to Triangular Plan Forms. NACA TN No. 1620, 1948.
3. Silverstein, Abe, Katzoff, S., and Bullivant, W. Kenneth: Downwash and Wake Behind Plain and Flapped Airfoils. NACA Rep. No. 651, 1939.
4. Hilton, W. F.: Measurement of Supersonic Downwash Behind Two Wings of Finite Span. Johns Hopkins University Applied Physics Laboratory. Rep. No. APL/JHU/CM-391, June, 1947.
5. Deacon, P. O.: Report on Wind Tunnel Tests of STV-2 Wing. Johns Hopkins University Applied Physics Laboratory. Rep. No. APL/JHU/CM-377, Mar. 1947.
6. Van Dyke, Milton D.: Aerodynamic Characteristics Including Scale Effect of Several Wings and Bodies Alone and in Combination at a Mach Number of 1.53. NACA RM No. A6K22, 1946.
7. Frick, Charles W., and Boyd, John W.: Investigation at Supersonic Speed ( $M=1.53$ ) of the Pressure Distribution Over a  $63^\circ$  Swept Airfoil of Biconvex Section at Zero Lift. NACA RM No. A8C22, 1948.
8. Michels, Walter C.: Advanced Electrical Measurements. 2d ed. D. Van Nostrand Co., N. Y., 1943, p. 11.
9. Ferri, Antonio: Experimental Results With Airfoils Tested in the High-Speed Tunnel at Guidonia. NACA TM No. 946, 1940.
10. Nielsen, Jack N., Matteson, Frederick H., and Vincenti, Walter G.: Investigation of Wing Characteristics at a Mach Number of 1.53. III - Unswept Wings of Differing Aspect Ratio and Taper Ratio. NACA RM No. A8E06, 1948.





*All dimensions are in inches.*

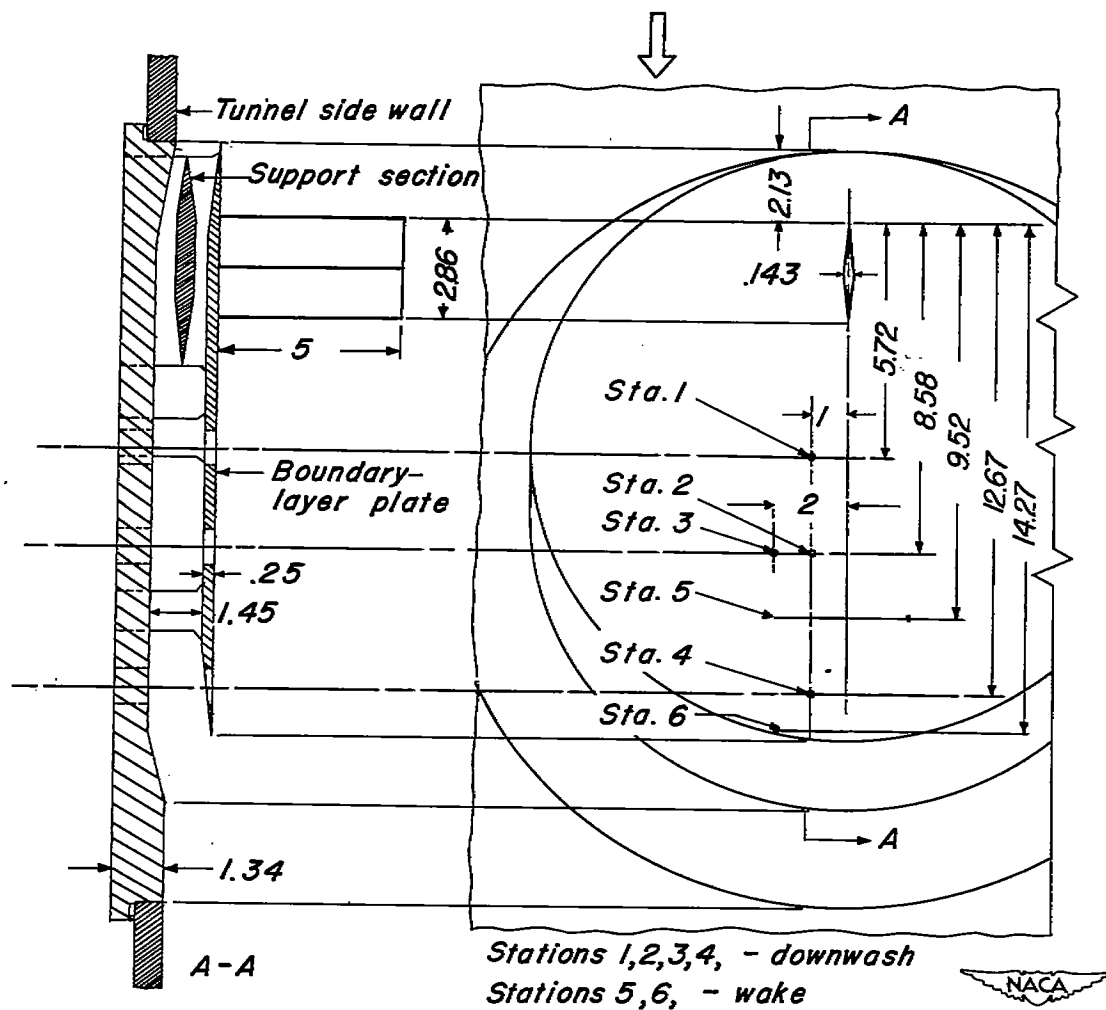
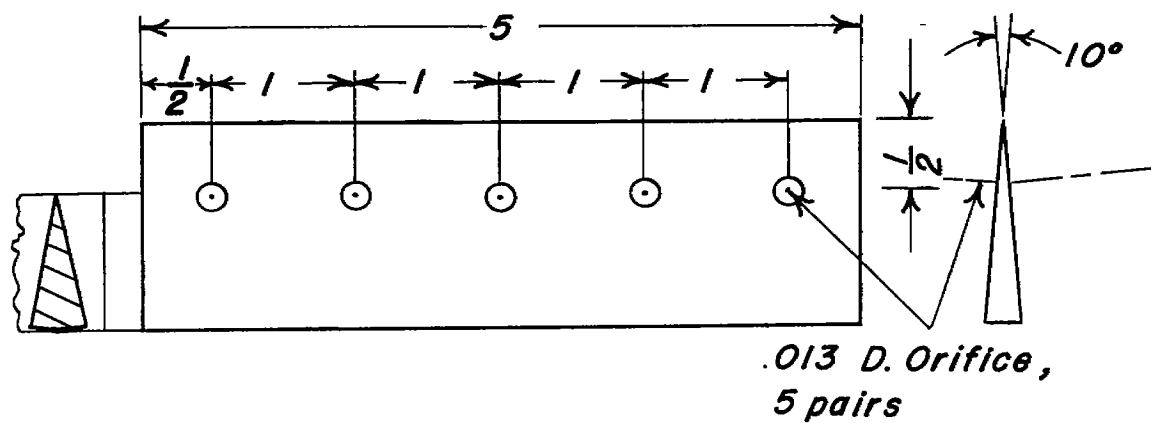
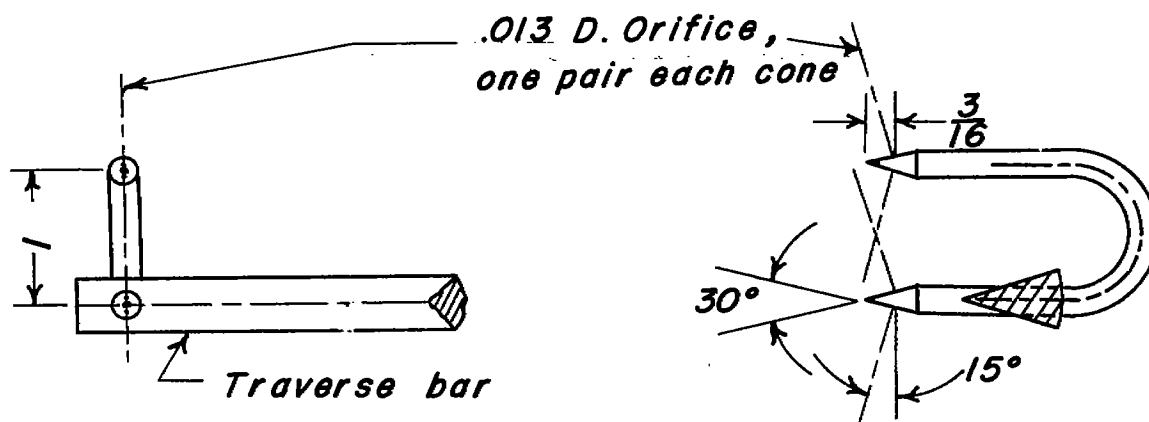


*Figure 1.—Sketch of model support system showing location of survey stations.*

*All dimensions are in inches except as noted.*



### *Wedge*

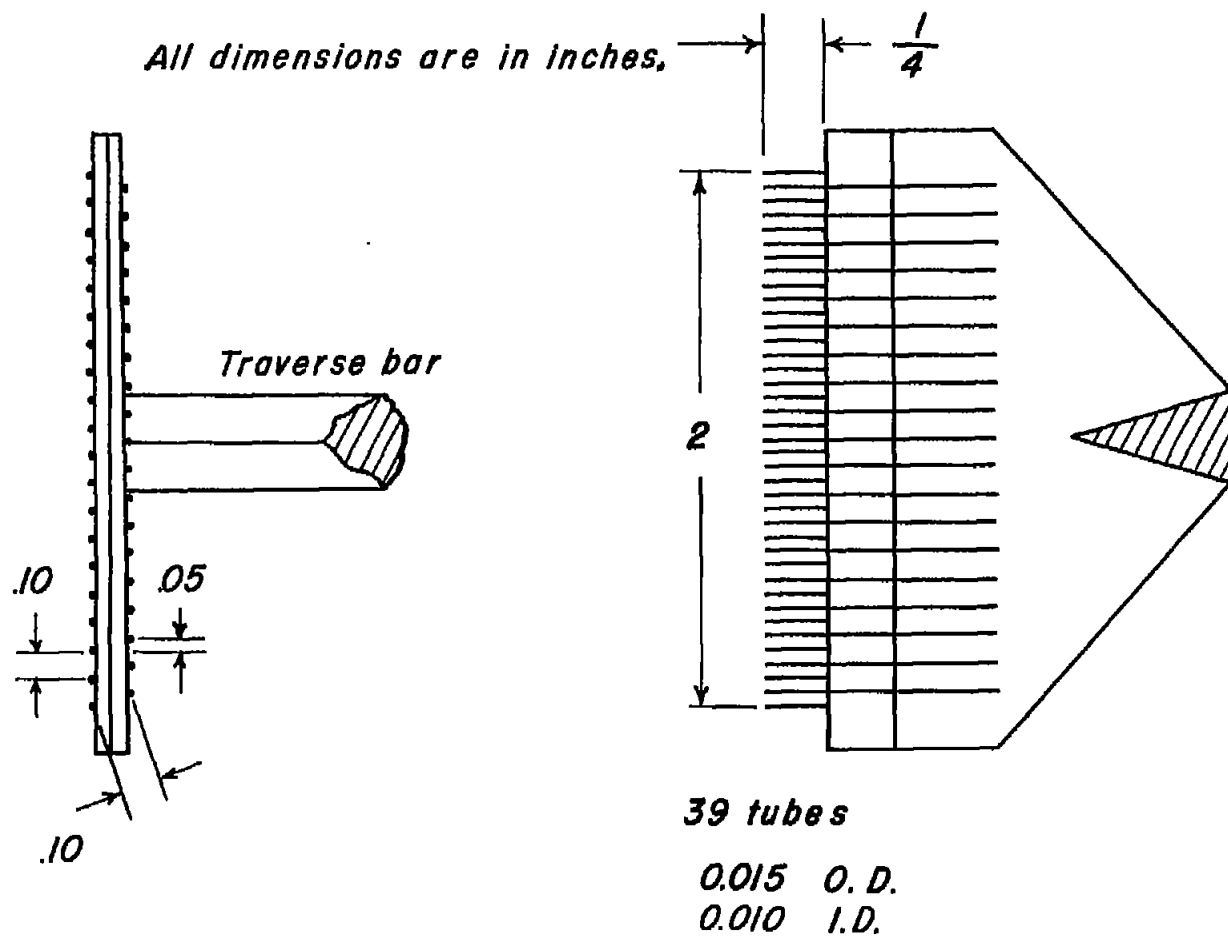


### *Cones*



*(a) Stream-angle instruments.*

*Figure 2.— Downwash and wake-survey instruments.*



*(b) Wake-survey rake.*

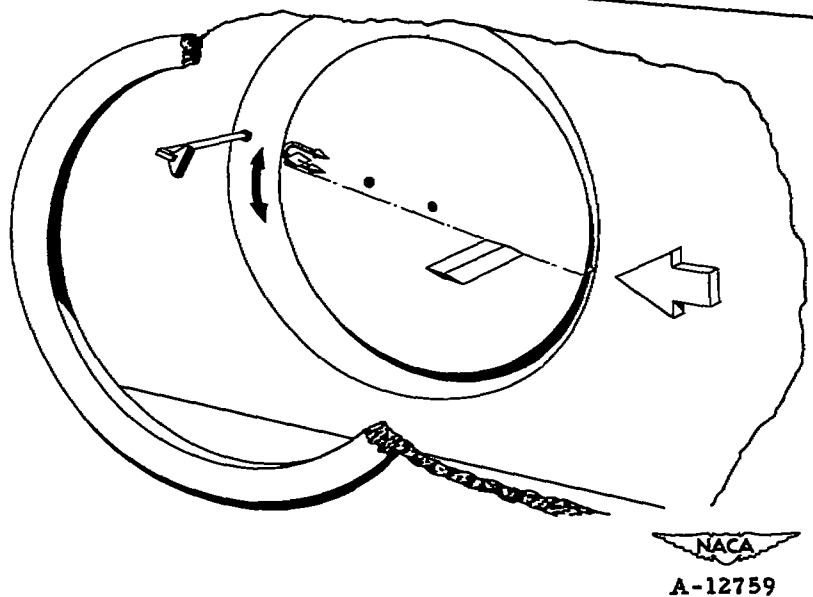
*Figure 2.—Concluded.*







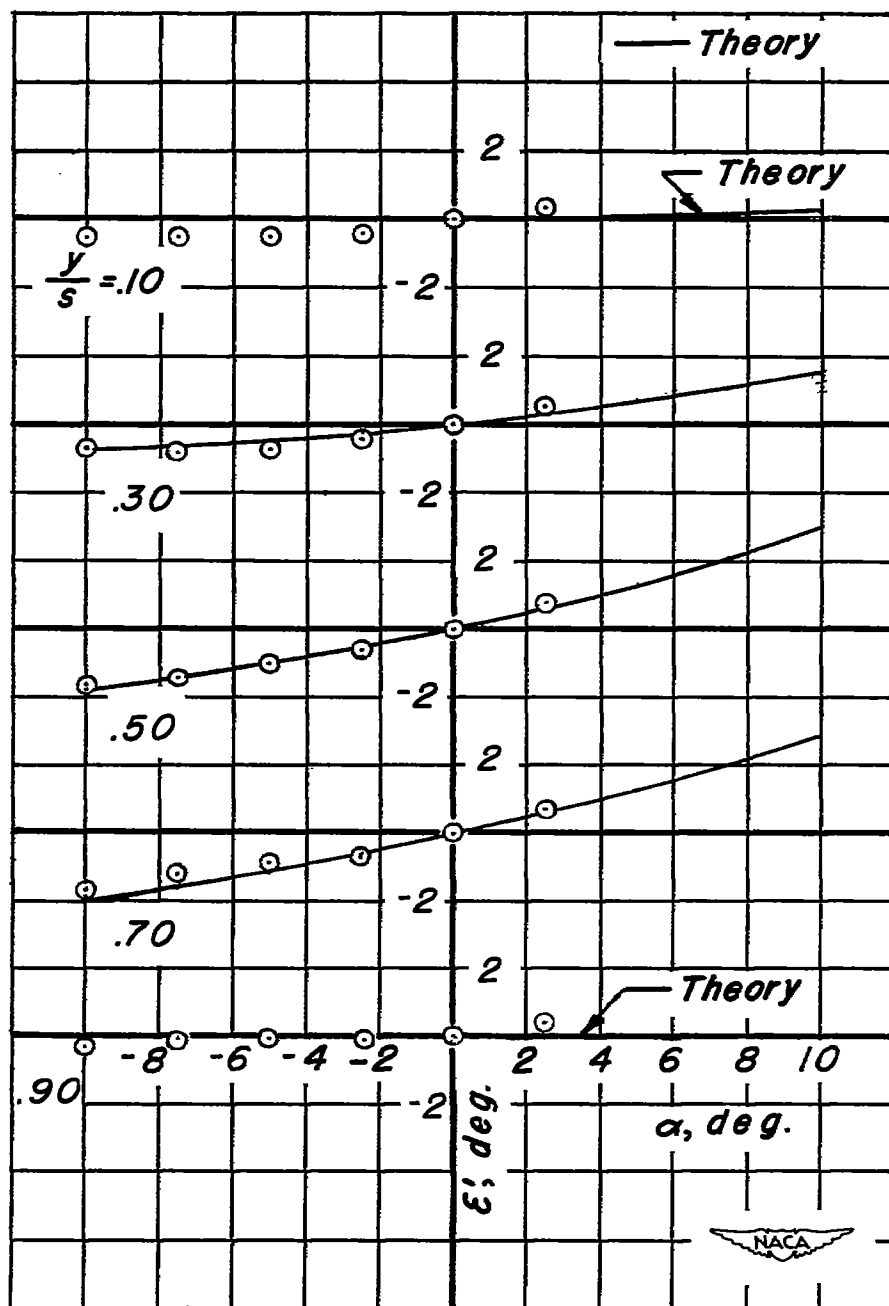
(a) Sketch showing the position of the wing and stream-angle wedge relative to the Mach cones which form the boundaries of the support interference region.



(b) Wing, stream-angle cones, and wake survey rake.  $\alpha \approx -10^\circ$ .

Figure 3.- Sketch of test section.

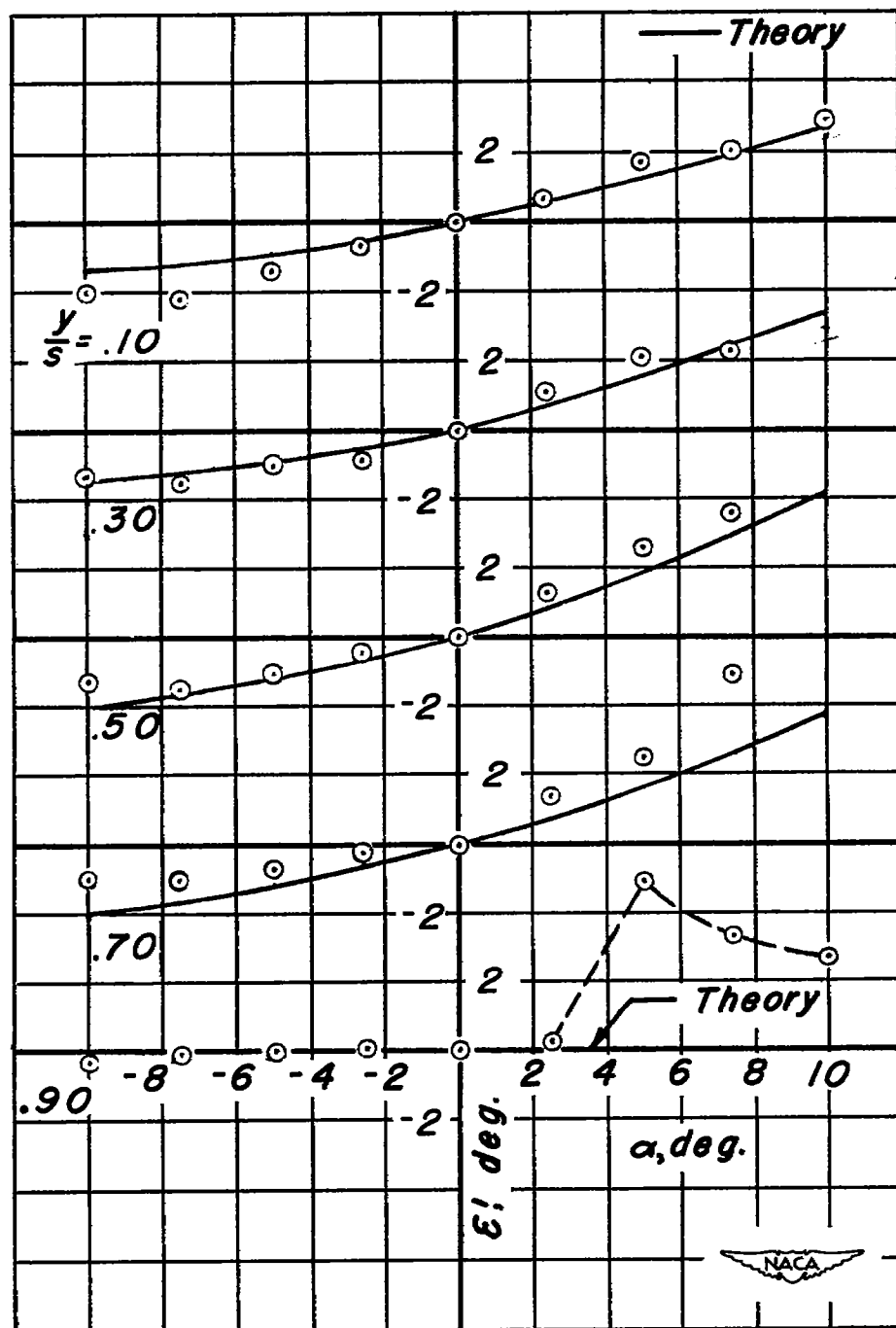




(a)  $x = 2c, z = 0.35c$ , Sta. I.

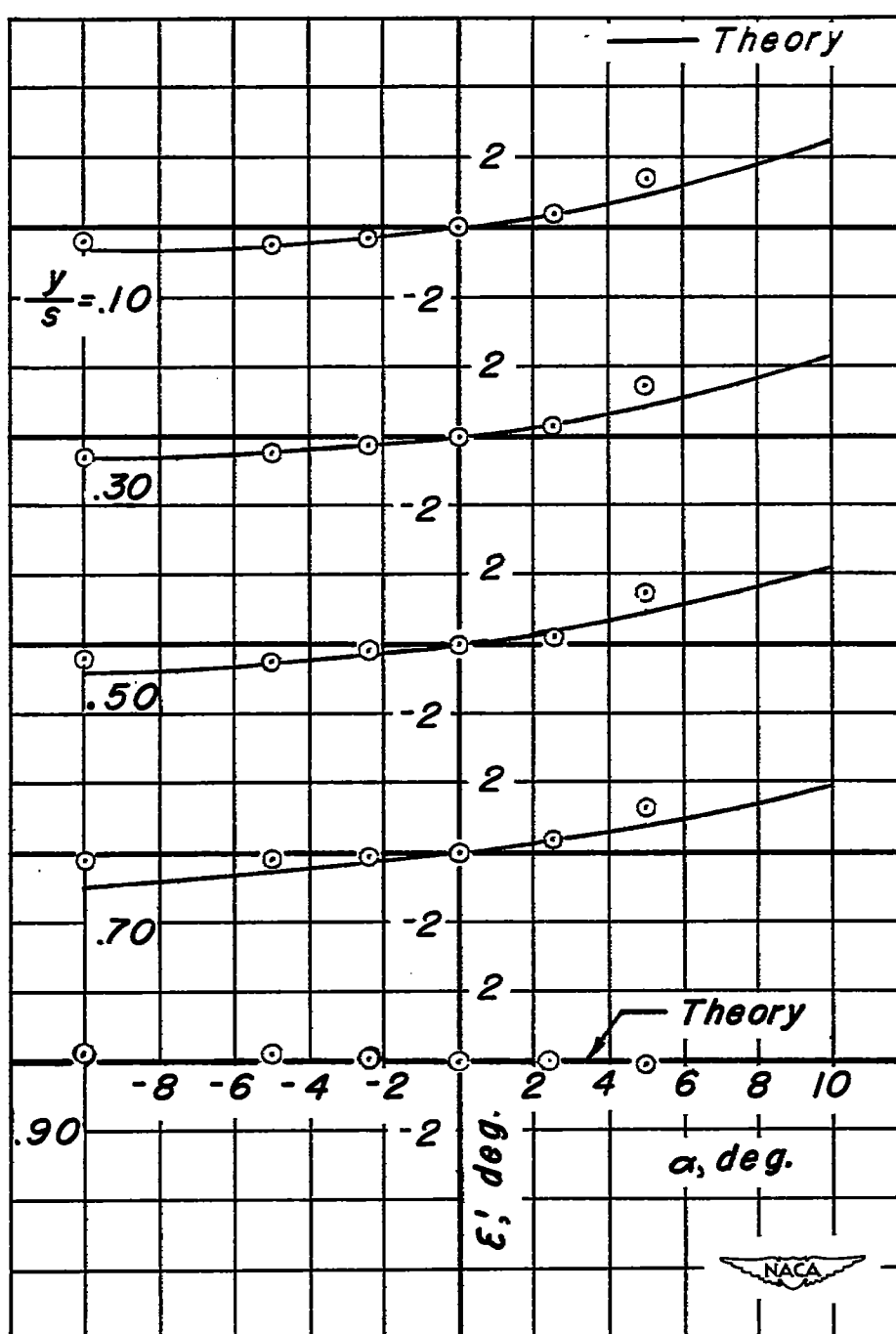
Figure 4.— Variation of downwash angle with angle of attack





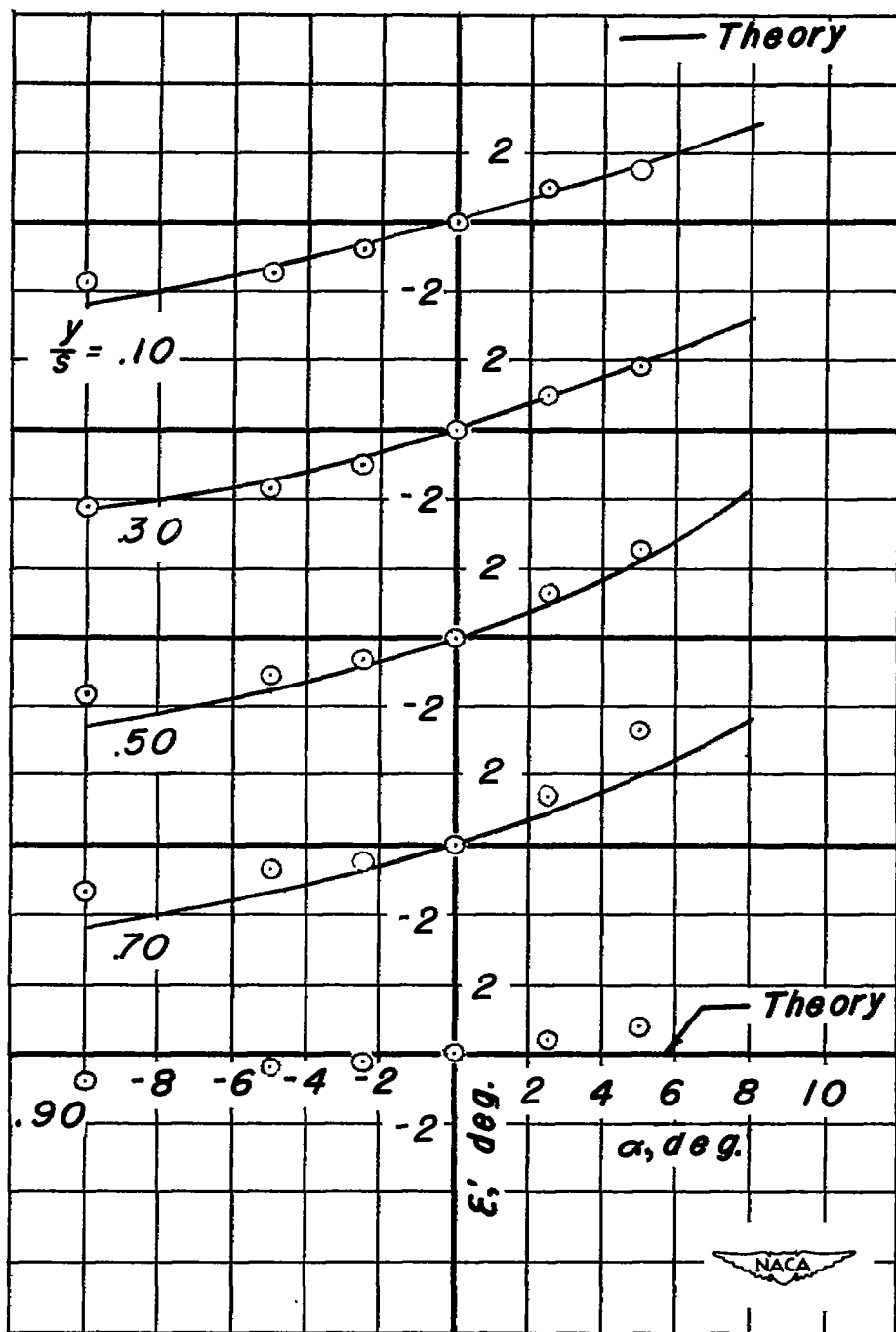
(b)  $x = 3c$ ,  $z = 0.35c$ , sta. 2.

Figure 4.-Continued.



(c)  $x = 3c$ ,  $z = 0.70c$ , sta.3.

Figure 4.—Continued.



(d)  $x = 4.43c$ ,  $z = 0.35c$ , sta. 4.

Figure 4.—Concluded.

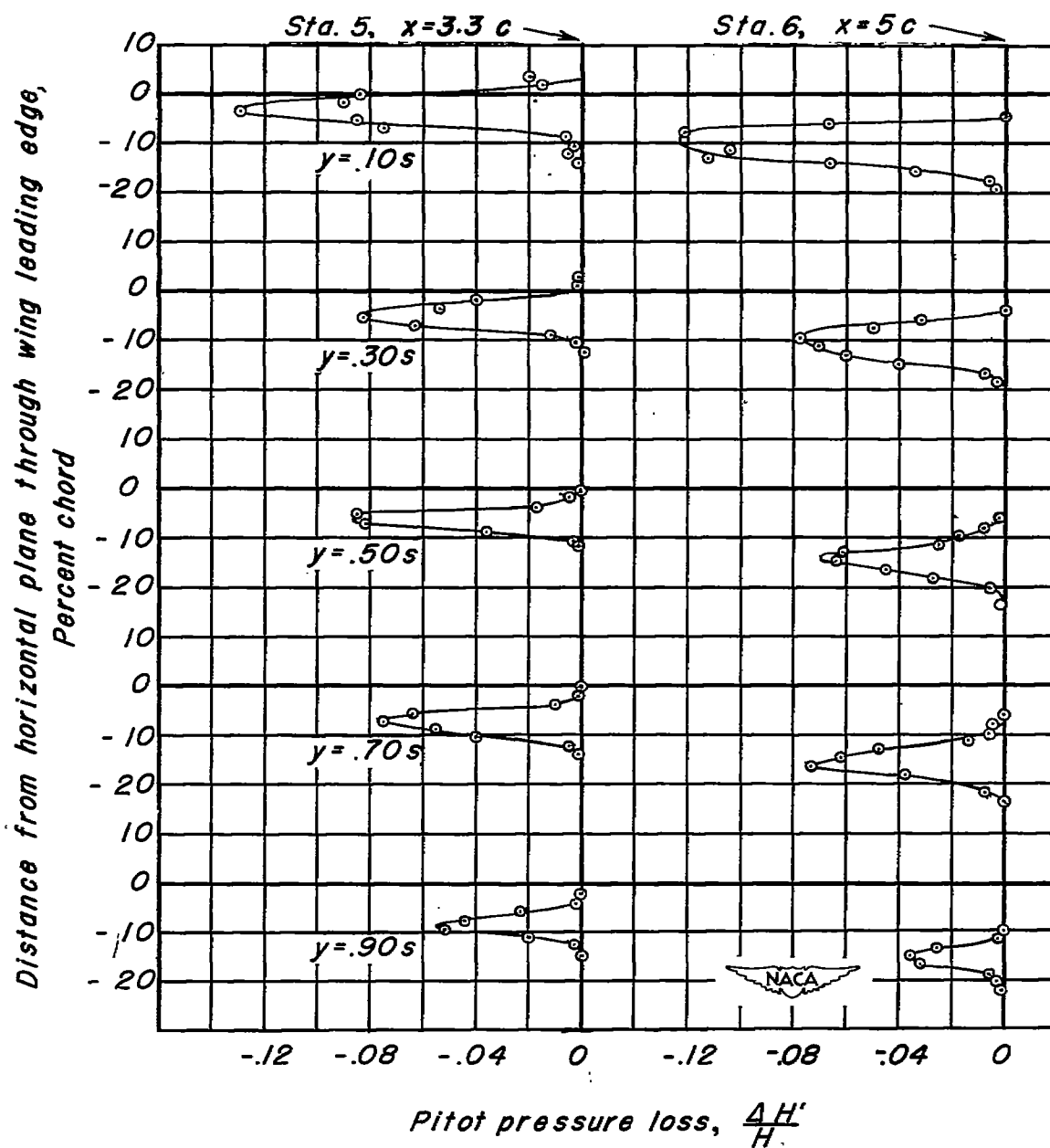


Figure 5.-Profiles of pitot pressure loss through viscous wake of rectangular wing.  $\alpha = 3^\circ$

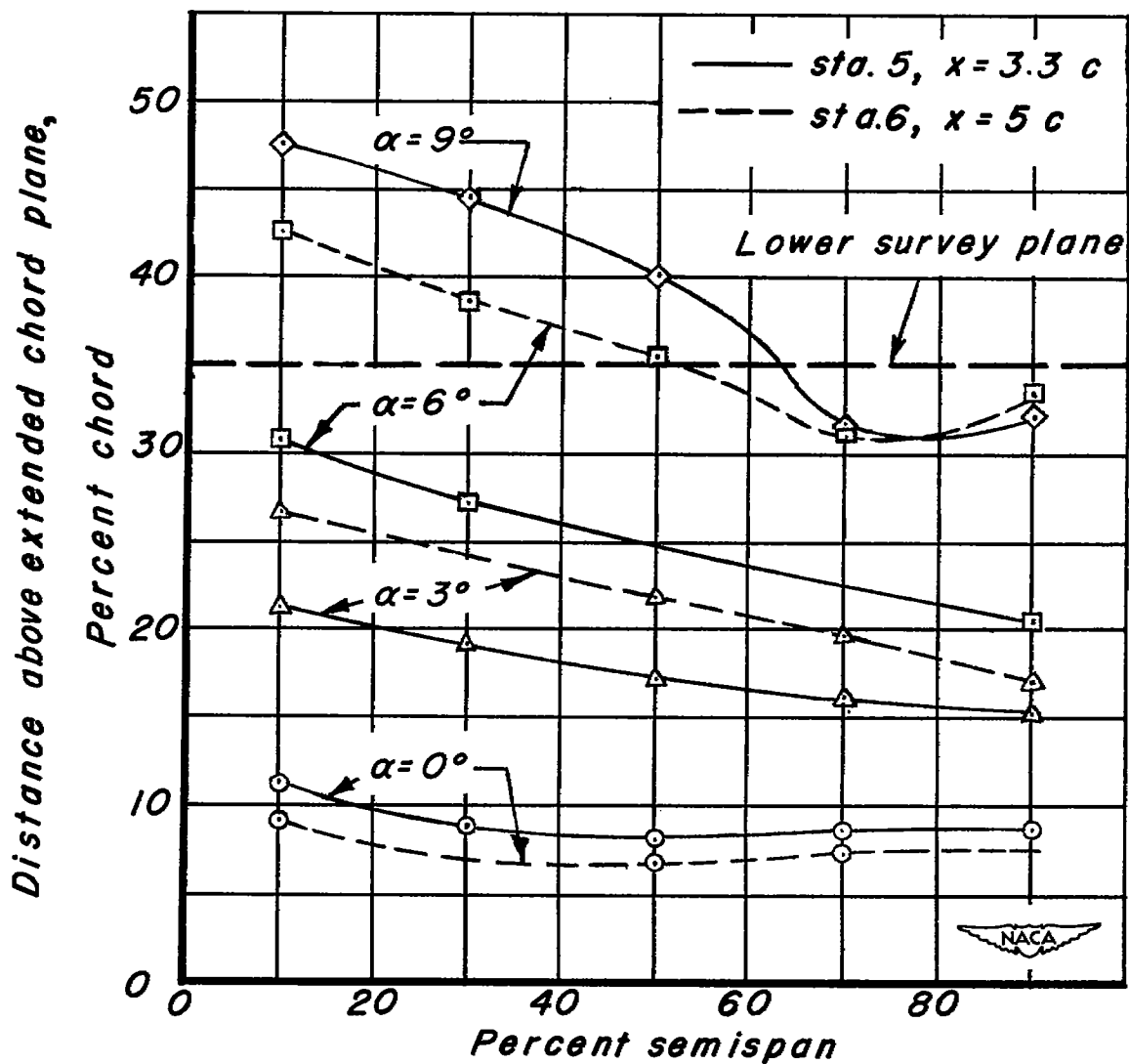


Figure 6.—Position of the upper limit of the viscous wake relative to the extended chord plane.

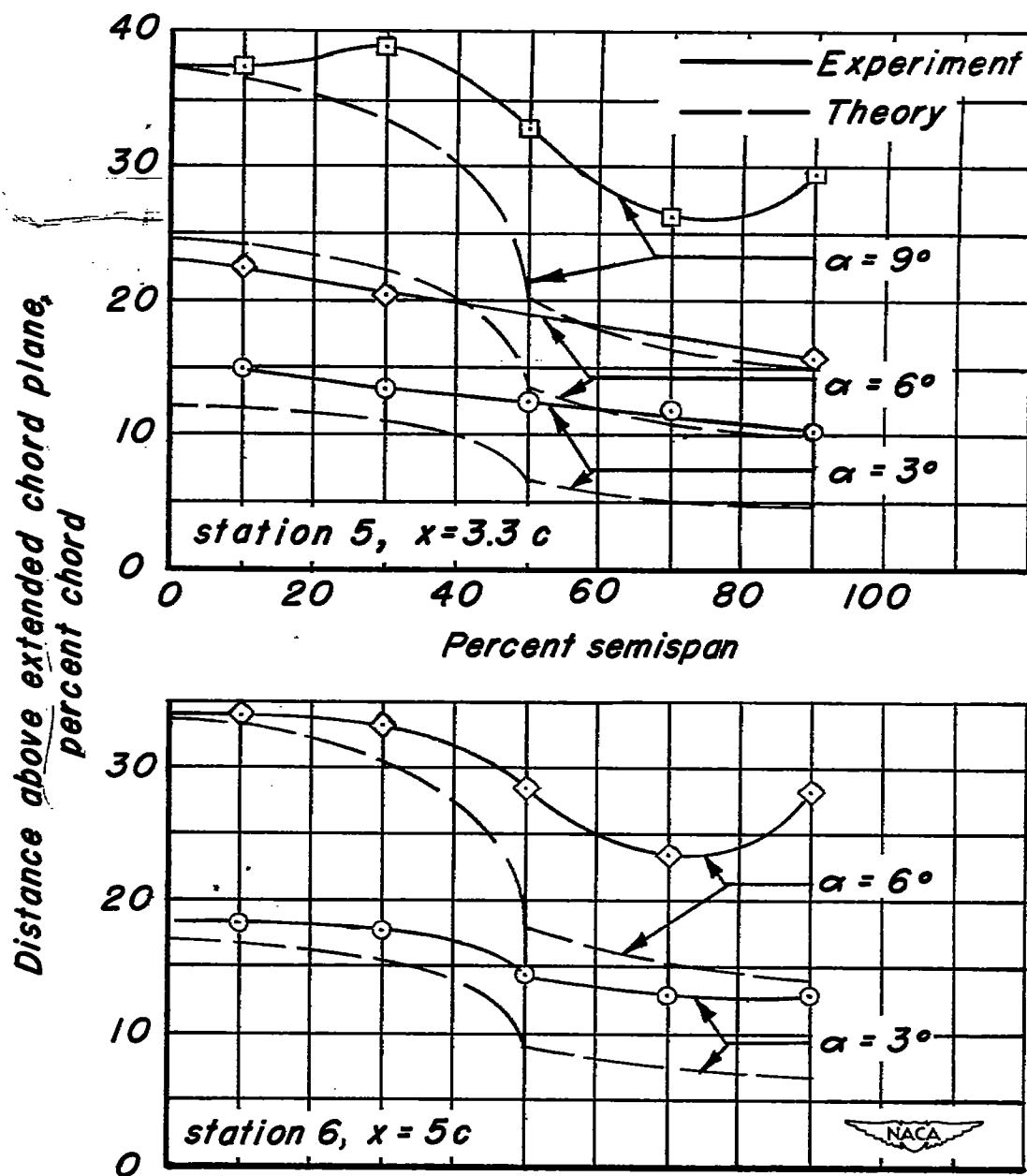


Figure 7.—Position of wake center line relative to extended chord plane.

NASA Technical Library



3 1176 01434 4700